
Statistical Modelling and predicting the Effects of Process Parameters in Flux Cored Arc Welding of AISI 301 Stainless Steel

By
M. V. Venkatesan¹, A. Manickavasagam² and A. Rajadurai³

^{1,2} Technical Training Centre, Integral Coach Factory, Chennai.

³ Madras Institute of Technology, Anna University.

ABSTRACT

Modelling is a technique widely used to represent the effect of multiple and interacting parameters on responses of many process. Welding is one such process where various parameters independently and interactively determine properties. The aim of this study is to reestablish the relationship between welding process parameters and tensile strength, slag inclusion count and penetration on the basis of statistical modelling. AISI 301 grade Stainless Steel Plates were welded with different CO₂ flow rates such as 10, 15 and 20L/min.

Visual test indicated that regularity of weld bead profile decreased with increase of flow rate. Gamma Radiographic Test revealed that slag inclusion count increased with increase of flow rate. Tensile test indicated that ultimate tensile strength of the specimen decreased with increase of flow rate. Hardness Test indicated that hardness of the specimen increased with increase of flow rate due to faster cooling rate. Micro structure analysis revealed that Heat affected zone of the specimen welded with 15 and 20 L/min have coarse and fine grained structure. Modelling equations were developed and can effectively be used to predict the slag inclusion count, tensile strength and penetration in terms of process parameters.

INTRODUCTION

Consumption of stainless steel is on the increase due to its excellent corrosion resistance property. Though Gas Tungsten Arc Welding (GTAW) process gives sound weldment, it has been limited due to its low deposition rate. As an alternate to GTAW process Flux Cored Arc Welding (FCAW) combines the benefit of both Shielded Metal Arc Welding (SMAW) process and Gas Metal Arc Welding process, and gives high deposition rate and improved physical properties of weldment.

COACH BUILDING

Over the past fifty years integral Coach Factory has been involved in fabrication of various types of coaches. Welding plays major role in fabrication of coaches. Corrosion of coaches is a major challenge to coach building. Toilets and adjoining areas are highly prone to corrosion and water percolation is more at trough floor and under frame. Initially Corten Steels were used for fabrication of trough floors there were not able to resist corrosion and frequent replacements were required. In order to check corrosion, Corten Steels are replaced by AISI 301 Stainless Steel and welded by E309 LT-1 Electrode, with Co₂ shielding gas.

OBJECTIVES

The specific objectives of the present study are

1. Finding the effect of the flow rate on weld bead profile, penetration pattern, slag inclusion count, tensile strength, hardness, composition and micro structure of the weldment.
2. Optimising the CO₂ flow rate for satisfactory weld joint.
3. Cost analysis.
4. Developing statistical model of process parameters.

MATERIALS AND METHODS

The composition of the base metal AISI 301 stainless steel and the filler metal 309LT-1 are listed in the Table 1.

Two grades of welders were subjected to the study. One is a qualified welder with weaving Bead method and other is an apprentice welder with stringer bead. The purpose was to check the reliability of the test results using a qualified welder and a trainee apprentice welder.

WELDING PROCEDURE

The stainless steel specimens were prepared to the size of 5 x 125 x 250mm and welded by both Apprentice and Qualified welder. The flow rate of the CO₂ selected for this study were 20, 15 and 10L/min. The specimens were butt welded in down hand (IG) position. The selected parameters are listed in the Table 2.

RESULTS

The welded specimens were subjected to visual inspection, gamma radiographic test, hardness test, tensile test and micro structure analysis. Weld pads welded with different flow rates were subjected to spectro test and compositions were found.

VISUAL INSPECTION

The overall qualitative assessment made on the appearance of the weldment by Visual Inspection is summarised and listed in the Table 3. The Visual Inspection indicated that irregularity of the weld bead increases with increase of CO₂ flow rate. The specimens welded with flow rates of CO₂ shielding gas ranging between 0-20 L/min resulted good penetration. This indicates that the quantity of CO₂ did not have any significant effect on penetration.

GAMMA RADIOGRAPHIC TEST

Specimens welded with different flow rates such as 20, 15 and 10 L/min by qualified and apprentice welder were subjected to gamma radiographic test. iridium 192 source was used and the specimen was exposed for 2 minutes. The number of slag inclusions present in a length of 250 mm of weldment were counted as slag inclusion count. The observation of the gamma radiographic test are listed in Table 4.

It is evident that the slag inclusion count increases as the CO₂ flow rate increases and this could be attributed to both the fast cooling of the weld pool as well as the high pressure exerted by the abduently flowing CO₂ gas. These two effects delayed the flotation of slag to the top layer of the weld pool and hence resulted increased slag entrapment. However it is important to note that if additional shielding with CO₂ gas is not provided, then surface porosities are observed due to insufficient protection to

the weld pool. Therefore it becomes essential to provide additional shielding with optimized flow of CO₂.

TENSILE TEST

The specimens welded with different flow rates were subjected to tensile test. The ultimate tensile strength (UTS) values are listed in Table 5. All the specimens failed at weldment. Test results indicated that tensile strength of the specimens decreased with increase of flow rate due to increase of slag inclusion count.

It is to be borne in mind that though the UTS values of the weld specimens decrease with increase in flow rate, the specimens welded without any shielding gas resulted large size surface porosity and the weldment become unfit for tensile test. The present specification for a quality weld is 515 MPa and therefore it could be stated that using CO₂ flow rate of 10L/minute acceptable quality weld could be obtained irrespective of the capability of the welder.

HARDNESS TEST

Hardness test results of welded specimens are listed in the Table 6. This test revealed that hardness is more at center of the weldment and hardness is reduced at weld toe and heat affected zone (HAZ). The increase in hardness value could be attributed to the occurrence of grain refinement due to faster cooling.

FRACTURE APPEARANCE

The specimens welded with the flow rates of 10 and 15L/min revealed the presence of few and many slag inclusions in the fractured surface respectively. (Figures 1 & 2)

CHEMICAL COMPOSITION

Chemical composition of the weld pad welded with different CO₂ flow rate such as 20, 15 and 10L/min are listed in the Table 7. It was observed that the

variation in the chemical composition of the weldment welded with different flow rates are negligible.

MICRO STRUCTURE OF THE WELDMENT

Fusion Zone (FZ): microstructure of the FZ revealed that the specimen welded with 20 and 10 L/min of flow rate has oriented delta ferrite and random oriented delta ferrite respectively. Specimen welded with 15L/min of flow rate revealed that transition from oriented to random delta ferrite and shown in the Figure 3(a-c) respectively.

HEAT AFFECTED ZONE (HAZ)

The microstructure of the HAZ revealed fine and coarse grain structure welded with the flow rate of 20 and 15L/min respectively and shown in Figs.4 & 5. The observed fine grain in heat affected zone is attributed to fast cooling due to higher flow rate.

COST ESTIMATION

Cost estimation is the process of calculating, the expenses, that must be incurred to manufacture the product. In this study cost estimations carried out for welding of stainless steel trough floor by flux cored wire with CO₂ shielding gas for both the existing and proposed flow rates.

UNIT CONVERSION

Weight of CO₂ cylinder : 31 kg
Density of CO₂ gas : 1.98
Volume of CO₂ gas : $V = M/D$
= 31/1.98
= 15.4 m³

TIME STUDY

Total length of weld = 60,000 mm
Length of weld done / min = 200 mm
Time taken to weld one frame = 300 min

VOLUME OF GAS REQUIRED / FRAME

Existing flow rate

of CO₂ gas = 20 L/min

Volume of gas required / frame

$$= 20 \text{ L/min} \times 300 \text{ min} : 6 \text{ m}^3$$

Volume of gas required for

1200 frames = 7200 m³ = 467.5 cylinder

(Approx 500 cylinder)

Existing consumption of cylinder for

1200 = 500 Nos.

frames with 20L/min

Proposed consumption of cylinder for

1200 frames with 10L/min.

$$= 250 \text{ Nos.}$$

Cost saving % = $\frac{500-250}{500}$

$$= 50\%$$

Saving Potential : 250 x 300

$$= \text{Rs.}75,000$$

STATISTICAL MODELLING

The study was carried out using the following steps:

1. Identifying the control variables and selecting their limits.
2. Development of experimental design matrix.
3. Conducting the experiments as per design matrix.
4. Recording the responses.
5. Developing the mathematical models.
6. Testing the significance of the coefficient by using, analysis of variance (ANOVA) technique and arriving at the final mathematical model.
7. Checking the adequacy of the developed model by correlation coefficient.

CONTROL VARIABLES

The independently controllable five predominant process parameters were identified and the selected limits are listed in the Table 8. The experimental design matrix is given in Table 9.

RESPONSE SURFACE METHODOLOGY

Response surface methodology (RSM) is a collection of mathematical and statistical technique that are for modeling an analysis of problem in which the response of interest (Y) is influenced by several variables (x) The function is denoted by

$$Y = f(x_1, x_2, x_3, x_4, x_5) + E$$

Where E Error observed in the response for the present study on representing the response output by 'R' the function can be expressed as $R = f(W, F, T, E, R)$.

The response variables are TS, SI, PN.

The model selected includes the effect of main variables and first order interaction of all variables. It is expressed as

$$\begin{aligned} \text{TS, SI, PN} = & b_0 + b_1W + b_2F + b_3WF \\ & + b_4T + b_5WT + b_6FT \\ & \dots b_{31} W.FTER. \end{aligned}$$

The higher order interactions are practically insignificant, so in this study only first and second order interactions were considered.

$$\begin{aligned} \text{TS, SI, PN} : & b_0 + b_1W + b_2F + b_3WF \\ & + b_4T + b_5WT + b_6FT \\ & + b_7TE + b_8WE + b_9FE \\ & + b_{10}TE + b_{11}R + b_{12}WR \\ & + b_{13}FR + b_{14}TR + b_{15}ER \end{aligned}$$

FINDING THE SIGNIFICANT FACTORS:

The yate's algorithm is used to find the Sum of Squares (SS) for main and interaction effect and analysis of variance (ANOVA) method is used to find the significant and interaction factors.

YATE'S ALGORITHM:

Tables 10, 11 & 12 list the SS values calculated using yate's algorithm. The experimental conditions and the corresponding totals are listed in standard order. In the column marked(1) the upper half is obtained by adding successive pairs of treatment totals and the lower half is obtained by subtracting the successive pairs. The same procedure was repeated to columns 2, 3, 4 and 5 and in column (SS) is obtained by squaring the corresponding effect total and then dividing the result by $r \times 2^n$. Where r is the number of trails and n is the number of process parameters for this present study $r = 1$ and $n = 5$.

ANALYSIS OF VARIANCE (ANOVA)

Using ANOVA 'F' values are predicted for tensile strength, slag inclusion count and penetration.

Evaluation of Coefficient of the model.

The final modeling equation for TS, SI and PN are

$$\begin{aligned} \text{TS} &= b_0 + b_1W + b_2F + b_3T + b_6WF \\ \text{SI} &= b_0 + b_1W + b_2F + b_3T + b_4E + b_6WF \\ \text{PN} &= b_0 + b_4E + b_5R \end{aligned}$$

All the other co-efficient are calculated by using the equation.

$$b_i = \frac{\sum x_i Y_i}{N}$$

i varies from 1 to N

Here 'X_i' is the corresponding coded values of the process parameters and Y_i is the corresponding values obtained from the experiment and 'N' is the No. of treatment combination considered (i.e.) 32.

FINAL MODEL

The final mathematical modeling equations developed from the above analysis to predict the TS, SI, PN of welded stainless steel plates by flux cored wires one given below:

$$SI = b_0 - 2.46W + 1.59F - 1.156T - 1.53WF + 0.09E$$

$$TS = b_0 + 22.59W - 11.09F + 13.40WF - 0.5313T$$

$$PN = b_0 + 7.8123E + 10.93R$$

Checking the adequacy of the developed modeling equations.

To coefficient of correlation (r) is used to find, how close the expected and observed values lie. The correlation co-efficient (r) is calculated by

$$r = \frac{(x-x)(y-y)}{(x-x)^2 (y-y)^2}$$

x = observed values for the response variables from the experiments.

y = Expected values for the response variable from the experiments.

x = Average observed response variable value

y = Average expected response variable value.

The calculated correlation co-efficient (r) for Tensile Strength is given in Table 13. Similarly the 'r' is calculated for slag inclusion count (SI) and penetration (PN)

CONCLUSION

An attempt was made to study the effect of the flow rate of CO₂ shielding gas on visual, radiographic quality, the tensile strength, micro structure, hardness and the nature of tensile fracture surface of AISI 301 stainless steel weldments made with FCAW process and statistical modeling equations were developed and the conclusion are as follows:

1. Welding of AISI 301 stainless steel plates of thickness 5mm without CO₂

shielding gas resulted incomplete penetration, porosity and poor quality bead geometry.

2. Welding of AISI 301 stainless steel sheets of thickness by a qualified welder with 10L/min of CO₂ gas results good penetration and UTS value of 568MPa.
3. Welding with CO₂ gas flow rate of 10L/min by apprentice welder resulted scattered presence of slag inclusion in the weldment and the UTS value was found to be 544MPa.
4. The quantity of slag inclusion increases with increase in the flow rate of CO₂ gas.
5. The presence of slag inclusion in large quantity decreases the UTS to low value of 490 MPa in the case of welding with CO₂ gas flow rate of 20L/min by apprentice welder.
6. CO₂ gas pushes the slag into the molten metal, thus slag entrapment into the weld bead increases with increase of CO₂ flow rate.
5. The presence of slag inclusion in large quantity decreases the UTS to low value of 490 MPa in the case of welding with CO₂ gas flow rate of 20L/min by apprentice welder.
6. CO₂ gas pushes the slag into the molten metal, thus slag entrapment into the weld bead increases with increase of CO₂ flow rate.
7. Manipulation of welding torch by stringer bead method increase the slag inclusion. Instead, in weaving bead method concentration of gas at the particular point is reduced. Hence weaving bead method is best

for welding of stainless steel by flux cored wire and decreases slag inclusion.

8. Microstructure of weldment consists of 10% of delta ferrite with austenite matrix.
9. Microstructure of weldment with 10L/min of CO₂ gas flow rate has random oriented delta-ferrite whereas the microstructure of weldment with 20L/min of CO₂ gas flow rate has preferred oriented delta-ferrite.
10. The application of qualified welder and apprentice welder did not show any significant change in test values.
11. The developed modeling equation can effectively be used to predict the tensile strength, slag inclusion in terms of process parameters obtained from any combination with in the range of variables studied for welding of stainless steel by flux cored wire.
12. The correlation coefficients for tensile strength, slag inclusion count and penetration are, 0.60, 0.55 and 0.56 respectively. It indicates good degree of agreement between experimental and predicted values.
13. Cost analysis indicated a 50% saving in the cost of CO₂ which works out to be about Rs.75,000/- for welding of 1200 under frames.

REFERENCE

1. Larry Jeffus, "Welding principles and application", Thosmas Delmar learning, U.S.A., 2004.
2. Sarma D.K., "Trends of Welding fabrication using cored wires" Indian Welding Journal, 2003, pp.47-55.

Element	C	Cr	Ni	Mo	Mn	Si	P	S	Cu
AISI 301	0.15	16-18	6-8	-	2.0	1.0	0.045	0.03	-
E309 LT-1	0.04	22.25	12.14	0.5	0.5-2.5	1.0	0.04	0.03	0.5

Table 1 : Chemical composition of Basemetal AISI 301 & Filler metal 309 LT-1 (Wt %)

Sl. No.	Parameter	Qualified welder	Apprentice
1.	Electrode size (mm)	1.2	1.2
2.	Current (amps)	160	140
3.	Voltage (volts)	28	24
4.	Polarity	DCRP	DCRP
5.	Edge preparations	Single 'V' included angle 60	Single 'V' included angle 60
6.	Welding technique	Fore hand	Fore hand
7.	Root gap (mm)	2.0	2.0
8.	Stick out (mm)	20-25	20-25

Table 2 : Welding process parameters

CO ₂ flow rate l/min	Porosity	Penetration pattern	Bead geometry
0	Observed	Incomplete penetration	Bad weld bead
10	Not observed	Good penetration	Regular weld bead
15	Not observed	Good penetration	Moderately regular
20	Not observed	Good penetration	Irregular

Table 3 : Visual Inspection Report

Sl. No.	CO ₂ flow rate	Qualified welder	Apprentice welder
1.	10	4	6
2.	15	5	15
3.	20	8	20

Table 4 : Gamma Radiographic Test Report

Sl. No	CO ₂ flow rate L/min	UTS Mpa	
		Qualified	Apprentice
1.	10	569	544
2.	15	565	466
3.	20	543	469

Table 5 : Tensile Test Report

Flow rate of CO ₂ gas (L/min)	Hardness (VHN)			
	Center of the weldment	Weld toe	HAZ1	HAZ2
10	391	362	345	340
15	405	396	367	362
20	407	396	386	367

Table 6 : Hardness Test Report

CO2 flow Rate (L/min)	% C	% Mn	% Si	% S	% P	% Cr	% Ni	% Cu	% Mo
20	0.049	1.32	0.66	0.006	0.022	22.03	12.15	0.12	0.09
15	0.049	1.25	0.66	0.006	0.021	22.04	12.19	0.12	0.09
10	0.046	1.30	0.66	0.006	0.021	22.05	12.11	0.13	0.09

Table 7 : Chemical composition the specimens welded with different flow rates

Parameters	Unit	Notation	Levels			
			Original		Coded	
			Low	High	Low	High
Welder	Wt factor	W	0.75	1.0	-1	+1
Flow Rate of CO2 gas	L/min	F	10	20	-1	+1
Thickness	mm	T	3	5	-1	+1
Edge preparation	Wt factor	E	0.5	1	-1	+1
Root Gap	Wt factor (mm)	R	0.5(1.2)	1(2)	-1	+1

Table 8 : Process parameters and their levels

Std Order	W (X ₁)	F (X ₂)	T (X ₃)	E (X ₄)	R (X ₅)	T.S (Mpa)	S.I (No)	PN %
1.	+1	+1	+1	+1	+1	543	8	100
2.	-1	+1	+1	+1	+1	469	20	80
3.	+1	-1	+1	+1	+1	569	4	100
4.	-1	-1	+1	+1	+1	562	6	80
5.	+1	+1	-1	+1	+1	540	8	100
6.	-1	+1	-1	+1	+1	469	18	100
7.	+1	-1	-1	+1	+1	540	8	100
8.	-1	-1	-1	+1	+1	530	10	90
9.	+1	+1	+1	-1	+1	569	5	70
10.	-1	+1	+1	-1	+1	543	7	70
11.	+1	-1	+1	-1	+1	570	4	60
12.	-1	-1	+1	-1	+1	540	8	100
13.	+1	+1	-1	-1	+1	562	6	100
14.	-1	+1	-1	-1	+1	469	15	100
15.	+1	-1	-1	-1	+1	540	9	100
16.	-1	-1	-1	-1	+1	530	10	100

Table 9 : Design Matrix

Std Order	W (X ₁)	F (X ₂)	T (X ₃)	E (X ₄)	R (X ₅)	T.S (Mpa)	S.I (No)	PN %
17.	+1	+1	+1	+1	-1	569	6	60
18.	-1	+1	+1	+1	-1	543	7	50
19.	+1	-1	+1	+1	-1	570	8	50
20.	-1	-1	+1	+1	-1	540	5	100
21.	+1	+1	-1	+1	-1	562	6	70
22.	-1	+1	-1	+1	-1	469	16	80
23.	+1	-1	+1	+1	-1	540	8	80
24.	-1	-1	-1	+1	-1	530	10	50
25.	+1	+1	+1	-1	-1	569	10	60
26.	-1	+1	+1	-1	-1	469	16	50
27.	+1	-1	+1	-1	-1	570	4	50
28.	-1	-1	+1	-1	+1	530	10	60
29.	+1	+1	-1	-1	-1	562	5	40
30.	-1	+1	-1	-1	-1	469	19	30
31.	+1	-1	-1	-1	-1	540	8	20
32.	-1	-1	-1	-1	-1	530	9	30

Table 9 : Design Matrix (contd.)

Sl. No.	Identif ication	Treatment Total	1	2	3	4	5	SS
1	1	8	28	38	82	146	293	2682.78
2	W	20	10	44	64	147	79	195.03
3	F	4	26	24	66	42	-51	81.28
4	WF	6	18	40	81	37	-53	87.78
5	T	8	12	26	26	-28	37	42.78
6	WT	18	12	40	16	-23	19	11.28
7	FT	8	21	40	10	-28	9	2.53
8	WFT	10	19	41	27	-25	-21	13.78
9	E	5	13	14	-26	22	-33	34.03
10	WE	7	13	12	-2	15	7	1.53
11	FE	4	22	6	-4	2	-1	0.031
12	WFE	8	18	10	-19	17	7	1.531
13	TE	6	26	-2	-18	8	-12	4.5
14	WTE	15	14	12	-10	1	-5	0.781
15	FTW	9	24	12	-12	-4	-2	0.125
16	WFTW	10	17	15	-13	-17	-17	9.03
17	R	6	12	-18	6	-18	-5	0.781
18	WR	7	2	-8	16	-15	5	0.781
19	FR	8	10	0	14	-10	5	0.781
20	WFR	5	2	-2	1	17	-7	1.531
21	TR	6	2	0	-2	14	15	7.031
22	WTR	16	4	-4	4	-15	-7	10531
23	FTR	8	9	-12	14	8	-12	4.5
24	WFTR	10	1	-7	3	-1	3	0.281
25	ER	10	1	-10	10	10	27	22.78
26	WER	16	-3	-8	-2	-13	-29	26.28
27	FER	4	10	-2	4	6	9	2.53
28	WFER	10	2	-8	5	-11	-23	16.53
29	TER	5	6	-4	2	-12	19	11.28
30	WTFR	19	6	-8	-6	10	-17	9.03
31	FTER	8	14	0	-4	-8	22	15.125
32	WFTER	9	1	-13	-13	-9	-1	0.031

Table 10 : Yate' S Algorithm To Calculate Ss For Slag Inclusion Count

Sl. No.	Identification	Treatment Total	1	2	3	4	5	SS
1	1	543	1012	2143	4222	8545	17107	9145295
2	W	469	1131	2079	4323	8562	-682	14535.13
3	F	569	1009	2222	4323	-280	312	3042
4	WF	562	1070	2101	4239	-402	342	3655
5	T	540	1112	2222	-207	174	-300	2812.5
6	WT	469	1110	2101	-73	138	30	28.13
7	FT	540	1031	2138	-159	120	10	3.13
8	WFT	530	1070	2101	-243	222	150	703.125
9	E	569	1112	-104	137	-142	16	8
10	WE	543	1100	-103	37	-158	50	78.13
11	FE	570	1031	-56	37	40	36	40.5
12	WFE	540	1070	-17	101	-10	70	153.125
13	TE	562	1038	-56	127	-18	184	1058
14	WTE	469	1100	-103	-7	28	46	66.125
15	FTW	540	1031	-140	79	40	36	40.5
16	WFTW	530	1070	-103	143	110	-102	325.125
17	R	569	-74	98	-21	100	16	8
18	WR	543	-7	39	-121	-84	122	465.13
19	FR	570	-71	-2	-121	134	36	40.5
20	WFR	540	-10	39	-37	-84	102	325.125
21	TR	562	-26	-2	1	-100	-16	8
22	WTR	469	-30	39	39	64	-50	78.13
23	FTR	540	-7	62	-47	-134	46	66.125
24	WFTR	530	-10	39	37	64	70	153.125
25	ER	569	-26	44	-59	84	-184	1058
26	WER	469	-30	83	41	100	218	1485.125
27	FER	570	-93	-4	41	-38	164	840.5
28	WFER	530	-10	-3	-23	84	198	1225.125
29	TER	562	-100	-4	39	100	16	8
30	WTFR	469	-40	83	1	-64	122	465.125
31	FTER	540	-93	60	87	-38	-164	840.5
32	WFTER	530	-10	83	23	-64	-26	21.125

Table 11 : Yate' S Algorithm To Calculate Ss For Tensile Strength

Sl. No.	Identif ication	Treatment Total	1	2	3	4	5	SS
1	1	100	180	360	750	1450	2330	169653.1
2	W	80	180	390	700	880	-50	78.125
3	F	100	200	300	540	-10	-30	28.125
4	WF	80	190	400	340	-40	70	153.125
5	T	100	140	210	-50	10	150	703.125
6	WT	100	160	330	40	-40	-70	153.125
7	FT	100	200	220	-40	30	-50	78.125
8	WFT	90	200	-120	0	40	-30	28.125
9	E	70	110	-40	-10	130	-250	1953.125
10	WE	70	100	-10	20	20	130	528.125
11	FE	60	170	40	-20	-10	30	28.125
12	WFE	100	160	0	-20	-60	10	3.125
13	TE	100	110	-10	-10	-30	-150	703.125
14	WTE	100	110	-30	40	-20	-90	253.125
15	FTW	100	70	20	40	-50	-30	28.125
16	WFTW	100	50	-20	0	20	-50	78.125
17	R	60	-20	0	30	-50	-570	10153.13
18	WR	50	-20	-10	100	-200	-30	28.125
19	FR	50	0	20	120	90	-50	78.125
20	WFR	50	-10	0	-100	40	10	3.125
21	TR	100	0	-10	30	30	-110	378.125
22	WTR	70	40	-10	-40	0	-50	78.125
23	FTR	80	0	0	-20	50	10	3.125
24	WFTR	80	0	-20	-40	-40	70	153.125
25	ER	50	-10	0	-10	70	-150	703.125
26	WER	60	0	-10	-20	-220	-50	78.125
27	FER	50	-30	40	0	-70	-30	28.125
28	WFER	60	0	0	-20	-20	-90	253.125
29	TER	40	10	10	-10	-10	-290	2628.125
30	WTFR	30	10	30	-40	-20	50	78.125
31	FTER	20	-10	0	20	-30	-10	3.125
32	WFTER	30	-10	0	0	-20	10	3.125

Table 12 : Yate' S Algorithm To Calculate Ss For Penetration

Sl. No.	X	(x - \bar{x})	Y	(y - \bar{y})	(x - \bar{x}) ²	(y - \bar{y}) ²	(x - \bar{x})(y - \bar{y})
1.	543	8.4	600.83	40	70.65	1600	336
2.	469	-65.6	513.12	-48	4303.33	2304	3149
3.	569	34.4	578.0	17	1183.4	289	59
4.	562	27.6	539	-22	762.0	484	-607
5.	540	5.4	602	41	29.2	1681	22
6.	469	65.6	529	-32	4303.0	1024	2099
7.	540	5.4	579	18	29.0	324	97
8.	530	-4.6	540	-21	21.0	441	97
9.	569	34.4	601	40	1183.4	1600	1376
10.	543	8.4	513	-48	70.6	2304	-403
11.	570	35.4	578	17	1253.16	289	602
12.	540	5.4	539	-22	29.16	484	-119
13.	562	27.4	602	41	750.76	1681	1123.4
14.	469	-65.6	529	-32	4303.36	1024	2099.2
15.	540	5.4	579	18	29.16	324	97.0
16.	530	-4.6	540	-21	21.16	441	97.0
17.	569	34.4	601	40	1183.36	1600	1376.0
18.	543	8.4	513	-48	70.56	2304	-403.2
19.	570	35.4	578	17	1253.16	289	602.0
20.	540	5.6	539	-22	31.36	484	-123.0
21.	562	27.4	602	41	750.76	1681	1123.4
22.	469	-65.6	529	-32	4303.36	1024	2099.0
23.	540	5.4	679	18	29.16	324	97.0
24.	530	-4.6	539	-22	21.16	484	101.0
25.	569	34.4	601	40	1183.36	1600	1376.0
26.	469	-65.6	556	-5	4303.36	25	328.0
27.	570	35.4	578	17	1253.16	289	6020
28.	530	-4.6	539	-22	21.16	484	101.0
29.	562	27.4	577	17	750.76	289	459.0
30.	469	-65.6	540	-29	4303.36	441	1378.0
31.	540	5.4	579	18	29.16	324	97.0
32.	530	-4.6	539	-22	21.16	484	101.0
	17107		17961		379851.3	28420	19418.0
Total	$\bar{x}=534.6$		$\bar{y} = 561$				

Table 13 : Correlation Co-efficient (r) For Tensile Strength

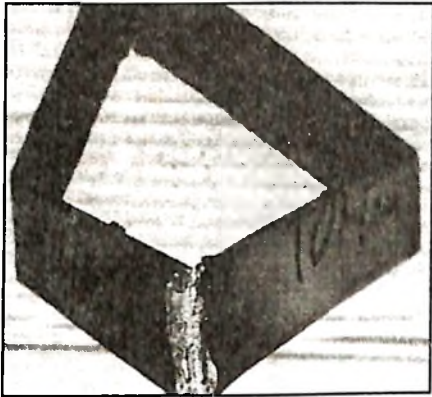


Figure 1 Fractured surface of the specimen welded with flow rate of CO₂ shielding gas - 10L/min

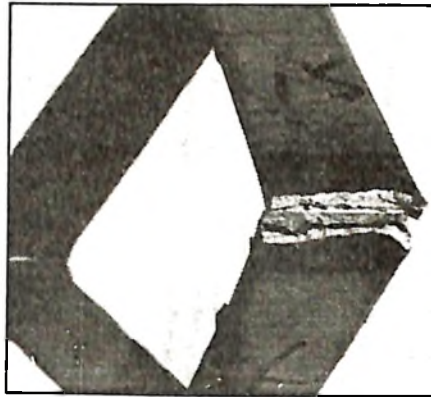


Figure 2 Fractured surface of the specimen welded with flow rate of CO₂ shielding gas - 15L/min



Figure 3a

Fig.3 Microstructure of the weld- ment welded with the flow rate 20, 15 and 10 L/min by qualified welder

a) 20L/min : Preferred orientation

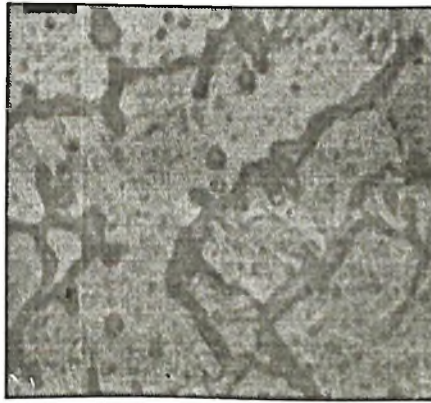


Figure 3b

b) 15L/min : Mixed orientation

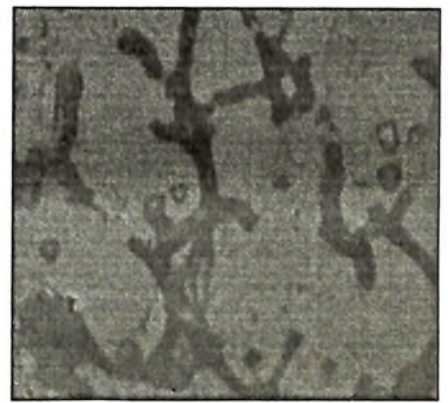


Figure 3c

c) 10L/min : Random orientation



Figure 4 Fine grain Flow Rate 20L/min



Figure 5 Coarse grain (Flow Rate 15L/min)